


Article

Simulation Calculation Verification of Graphene Oxide-Decorated Silver Nanoparticles Growing on Titania Nanotube Array as SERS Sensor Substrate

Yibing Xie 

School of Chemistry and Chemical Engineering, Southeast University, Nanjing 211189, China; ybxie@seu.edu.cn

Abstract: Graphene oxide-decorated silver nanoparticles growing on titania nanotube array (GO/Ag/TiO₂ NTA) were designed as active Surface-enhanced Raman scattering (SERS) sensor substrates for sensitive determination of the organic compound bisphenol A. The theoretical simulation calculation and experimental measurements have been adopted to investigate the electronic and sensing properties of GO/Ag/TiO₂ NTA SERS substrate. The molecule adsorption and surface energy are applied to investigate the interfacial interaction between the SERS substrate and the organic molecule. The Raman spectrum response intensity and the electron transfer behavior are applied to investigate sensing activity of GO/Ag/TiO₂ NTA SERS substrate. The specific adsorption amount of BPA is 3.3, 7.1, and 52.4 nmol cm⁻² for TiO₂, Ag/TiO₂, and GO/Ag/TiO₂ NTA, respectively, presenting superior adsorption and aggregation capability. GO/Ag/TiO₂ NTA SERS sensor accordingly achieves the low detection limit of 5×10^{-7} M for bisphenol A molecule. The density functional theory simulation calculation proves that GO/Ag/TiO₂ reveals a higher density of states, lower HOMO-LUMO gap, stronger electrostatic interaction, and similar band gaps in comparison with Ag/TiO₂. Binary-interfaced GO/Ag/TiO₂ presents a more declined molecule structure surface energy of 5.87 eV rather than 4.12 eV for mono-interfaced Ag/TiO₂. GO/Ag/TiO₂ also exhibits a more declined surface adsorption energy of 7.81 eV rather than 4.32 eV for Ag/TiO₂ in the adsorption of bisphenol A. The simulation calculation verification results well confirm the superior activity of GO/Ag/TiO₂ NTA substrate for sensitive detection and quantitative determination of the organic compound bisphenol A.

Keywords: SERS sensor substrate; simulation calculation; graphene oxide/silver/titania nanotube array; organic compound determination



Citation: Xie, Y. Simulation Calculation Verification of Graphene Oxide-Decorated Silver Nanoparticles Growing on Titania Nanotube Array as SERS Sensor Substrate. *Chemosensors* **2022**, *10*, 507. <https://doi.org/10.3390/chemosensors10120507>

Academic Editors: Shan Cong and Chunlan Ma

Received: 25 October 2022

Accepted: 26 November 2022

Published: 30 November 2022

Publisher's Note: MDPI stays neutral with regard to jurisdictional claims in published maps and institutional affiliations.



Copyright: © 2022 by the author. Licensee MDPI, Basel, Switzerland. This article is an open access article distributed under the terms and conditions of the Creative Commons Attribution (CC BY) license (<https://creativecommons.org/licenses/by/4.0/>).

1. Introduction

Surface-enhanced Raman scattering (SERS) is regarded as an ultrasensitive analytical method for molecular detection and determination [1]. A lot of preparation methods are reported to form SERS substrates, which include e-beam lithography, electrochemistry and laser ablation. These SERS substrates reveal great Raman signal stability and good detection limits that even allow detecting low concentrations down to single molecule level [2–6]. Raman enhancement mechanisms of the SERS effect include the electromagnetic enhancement and chemical enhancement [7]. Raman electromagnetic enhancement is achieved when the localized surface plasmon, excited from the surface of noble metal nanoparticles, generates a strong local electromagnetic field. Raman chemical enhancement is achieved by the charge transfer between the noble metal substrate and surface-adsorbed molecules [8]. SERS sensing performance is usually related to the hot spots of rough noble metals and the adsorption properties of organic molecules on noble metals. The nanostructured rough noble metals, such as Au or Ag nanoparticles, are regarded as effective SERS substrates. Titanium dioxide nanotube array (TiO₂ NTA) with high surface area has been proven to act as an effective supporting substrate to noble metal nanoparticles [9]. It has been reported

that Ag/TiO₂ with various structures has been developed as active SERS substrates for sensitive detection and accurate determination applications [10,11].

Concerning the Raman chemical enhancement effect, the interfacial affinity between SERS substrates and organic molecules plays an important role in influencing the Raman enhancement effect. The surface microstructure and adsorption properties of substrate materials highly affect SERS detection and determination performance [12,13]. The molecule 4,4'-(Propane-2,2-diyl)diphenol (Bisphenol A, BPA) with two hydroxyl groups has been regarded as a typical aromatic compound among various endocrine disruptors, which are used as representative organic compounds for SERS-sensing detection [14]. The SERS-sensing BPA molecule becomes invalid on the base of bare noble metal substrates since the BPA molecule has very low adsorption and aggregation properties. The interfacial interaction usually plays an important role in improving the activities of substrate materials [15,16]. Graphene oxide (GO) is used to dissolve the organic molecules with insufficient adsorption and low affinity onto the plasmonic noble metals. GO keeps oxygen-containing functional groups (such as epoxide, hydroxyl, carboxyl, and carbonyl groups) on the surface [17]. GO has a high adsorption capability toward organic aromatic compounds on the SERS substrate [18]. It was also reported that the graphene-modified SERS substrate is able to generate the SERS chemical enhancement effect [19,20]. An Ag/TiO₂ composite is suitable for SERS substrate application since both Ag and GO composites have SERS activity [21,22]. Our previous works had proven that GO modification of Ag/TiO₂ NTA could be used for SERS-sensing detection of organic aromatic ring molecules [23]. It is believed that GO/Ag/TiO₂ becomes a reasonable choice as a SERS substrate [24,25].

The theoretical basis is still sufficient to support high sensing performance of GO/Ag/TiO₂ SERS sensor substrate. The simulation calculation on the basis of the Density Functional Theory (DFT) is an effective approach to disclose the electronic properties, which are related to Raman electromagnetic enhancement, and the interfacial adsorption energy, which is related to Raman chemical enhancement [26–29]. In this study, GO-decorated Ag nanoparticles/TiO₂ nanotube arrays (GO/Ag/TiO₂ NTA) were designed as active SERS sensor substrates for sensitive detection and determination of the organic compound BPA. The experimental measurement and theoretical simulation calculation have been adopted to investigate the sensing properties of GO/Ag/TiO₂ NTA SERS substrate. The interfacial adsorption and interfacial energy are applied to investigate the interaction between the SERS substrate and the organic molecule. The Raman spectrum-response intensity and the electron transfer behavior are applied to investigate the sensing activity of the SERS substrate.

2. Experimental Measurement and Theoretical Calculation Section

2.1. Experimental Measurement and Characterization

Ag/TiO₂ NTA was fabricated by depositing Ag nanoparticles on the surface of TiO₂ NTA through a polyol reduction process, where TiO₂ NTA was immersed in a polyvinyl pyrrolidone, ethylene glycol, and water mixture solution containing AgNO₃ precursor. GO/Ag/TiO₂ NTA was fabricated by decorating Ag/TiO₂ with graphene oxide (GO) through an impregnation process, where Ag/TiO₂ NTA was immersed in GO aqueous solution; we then conducted a thermal treatment. The organic compound bisphenol A (BPA) was used as a probe molecule, and GO/Ag/TiO₂ NTA was used as the SERS substrate for the SERS sensor application. The surface adsorption between the GO/Ag/TiO₂ SERS substrate and the BPA molecule was investigated by UV-vis spectrometry. The SERS sensing of BPA was investigated through Raman spectrum measurements.

The surface microstructure characterizations of TiO₂, Ag/TiO₂, and GO/Ag/TiO₂ NTA were carried out by a Field Emission-Scanning Electron Microscope (FE-SEM, Zeiss Ultra-Plus, Oberkochen, Germany). UV-Vis absorption spectrum measurements were conducted by UV/Vis Spectrometer (Shimadzu UV-2100 UV/Vis Spectrometer, Kyoto, Japan). Raman spectrum measurements were conducted by Renishaw InVia Reflex System Raman spectrometer (London, UK).

2.2. Theoretical Calculation Section

The density functional theory (DFT) simulation calculation was applied to investigate the electronic properties of Ag/TiO₂ and GO/Ag/TiO₂ NTA SERS substrate. The interfacial adsorption interaction of Ag/TiO₂ and GO/Ag/TiO₂ with organic molecules was investigated. The total density of states (DOS), highest occupied molecular orbital (HOMO), lowest unoccupied molecular orbital (LUMO), charge density difference, Mulliken charge population, and interfacial binding energy were fully investigated for better understanding of the electrostatic interfacial interaction in the SERS substrates.

A detailed first-principles calculation was performed to investigate the electronic properties of GO/Ag/TiO₂. The DMol3 and CASTEP packages of Materials Studio were employed to perform geometry optimization and energy calculations. The dispersion-corrected density functional theory was utilized for structure optimization and energy convergence. In view of the exchange–correlation functional, the Perdew–Burke–Ernzerhof generalized gradient approximation was conducted via combination with Grime’s long-range dispersion correction. The wave functions of systems were described using the double numeric plus polarization basis set. The thresholds of the convergence tolerance included the following setup values: the convergence tolerance of the energy under 10^{−5} hartree (1 hartree = 27.21 eV) was 0.005 Å for the maximum allowable displacement and 0.002 hartree/Å for the maximal force. The 1 × 2 × 2 Monkhorst–Pack grid in the Brillouin zone was used, and a cutoff radius of 12.5 Å was applied. Furthermore, the systematically theoretical calculations, including energy gap, density of states (DOS), electrostatic potential (ESP), surface energy, and highest occupied molecular orbital to lowest unoccupied molecular orbital (HOMO–LUMO) gap, were performed to explore the electrical properties of GO/Ag/TiO₂.

3. Results and Discussion

Figure 1 shows the schematic diagram of the forming process of the GO/Ag/TiO₂ NTA SERS substrate and corresponding SEM microstructures of TiO₂, Ag/TiO₂, and GO/Ag/TiO₂ NTA. The forming process of GO/Ag/TiO₂ NTA is shown below. The Ag nanoparticles were well-dispersed on the surface of anatase TiO₂ NTA to form Ag/TiO₂ NTA. The surface of Ag/TiO₂ NTA was then decorated with GO to form GO/Ag/TiO₂ NTA. The adsorption capability and SERS sensing activity of the GO/Ag/TiO₂ NTA substrate were investigated for the detection and determination of bisphenol A (BPA).

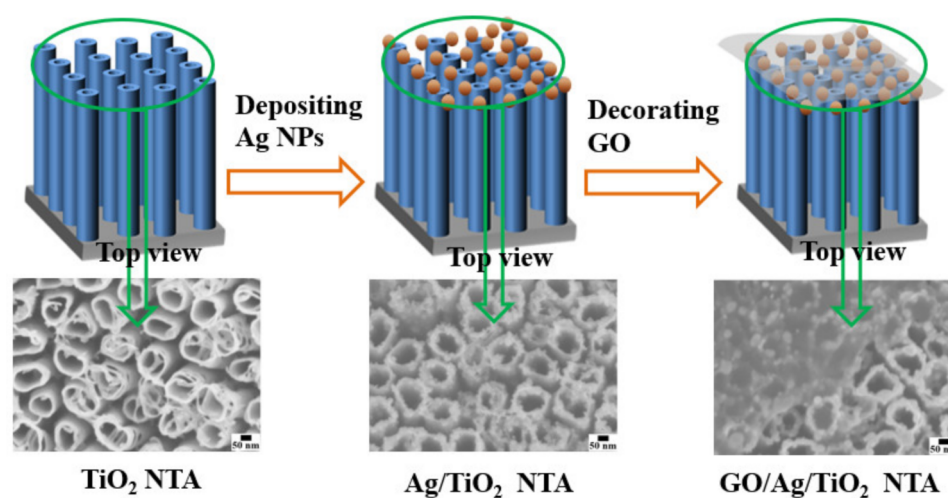


Figure 1. Schematic diagram of the forming process of GO/Ag/TiO₂ NTA SERS substrate and corresponding top view of SEM images of TiO₂, Ag/TiO₂, and GO/Ag/TiO₂.

Concerning the morphology of TiO₂, Ag/TiO₂, and GO/Ag/TiO₂ NTA shown in the top view of the SEM images, TiO₂ NTA exhibits highly ordered, vertically aligned nanotube microstructure. Ag/TiO₂ NTA shows that Ag nanoparticles are evenly dispersed on the

pore mouth of TiO₂ nanotubes. GO/Ag/TiO₂ NTA shows that the semi-transparent GO monolayer coats the top surface of Ag/TiO₂ NTA. The GO keeps semi-transparent covering layer structure. Such a GO layer induces the activation modification of Ag nanoparticles. Ag/TiO₂ keeps a mono interface and GO/Ag/TiO₂ keeps binary interfaces.

The Raman electromagnetic and chemical enhancements are highly related to the electronic structures of the SERS substrates. The DFT simulation calculation is applied as the effective and useful approach to investigate the interfacial electron transfer and charge distribution of the binary composite material of GO/Ag/TiO₂ [13,30]. Figure 2A,B show molecule structure models of Ag/TiO₂ and GO/Ag/TiO₂ SERS substrates. The molecular structure model of Ag/TiO₂ involves the mono interface, which is related to the {1, 0, 1} crystal lattice plane of anatase TiO₂ and the face-centered cubic crystal plane of Ag. The molecular structure model of GO/Ag/TiO₂ involves the binary interfaces of the as-described Ag/TiO₂ and GO/Ag, which are related to the sp²-hybridized hexatomic carbon ring of GO and the cubic crystal plane of Ag. Additionally, GO includes hydroxyl and epoxy functional groups distributed on the surface, which can conduct the interfacial interaction with Ag nanoparticles and the organic molecule BPA [22,31].

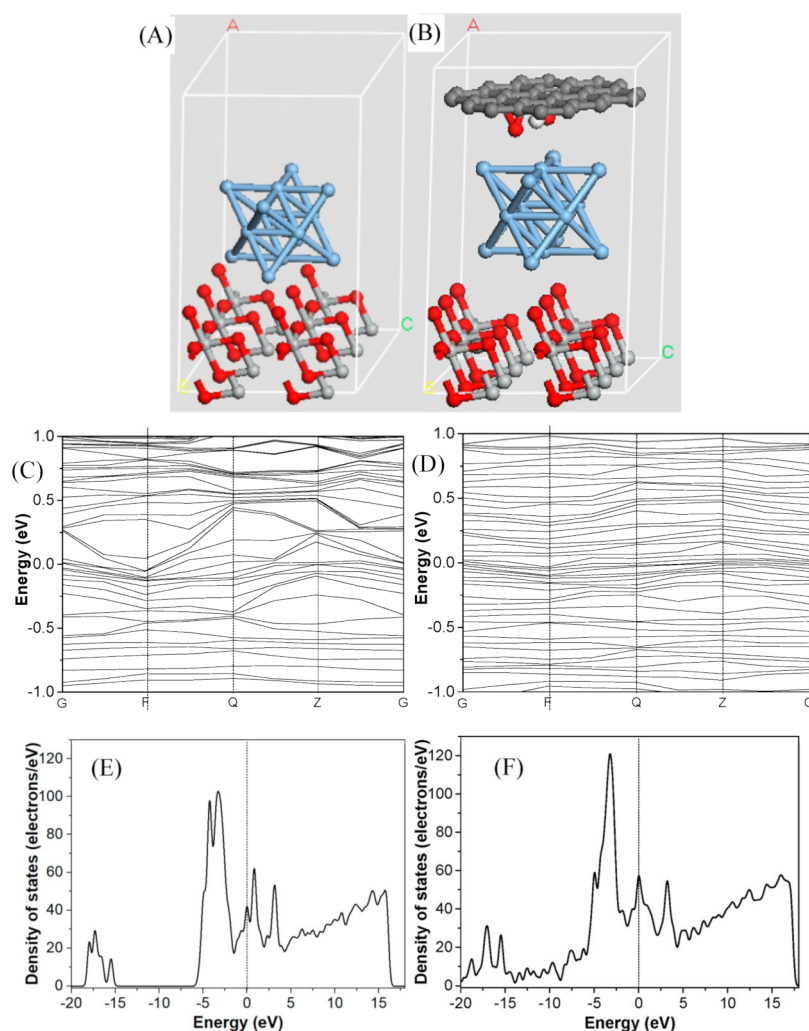


Figure 2. Cont.

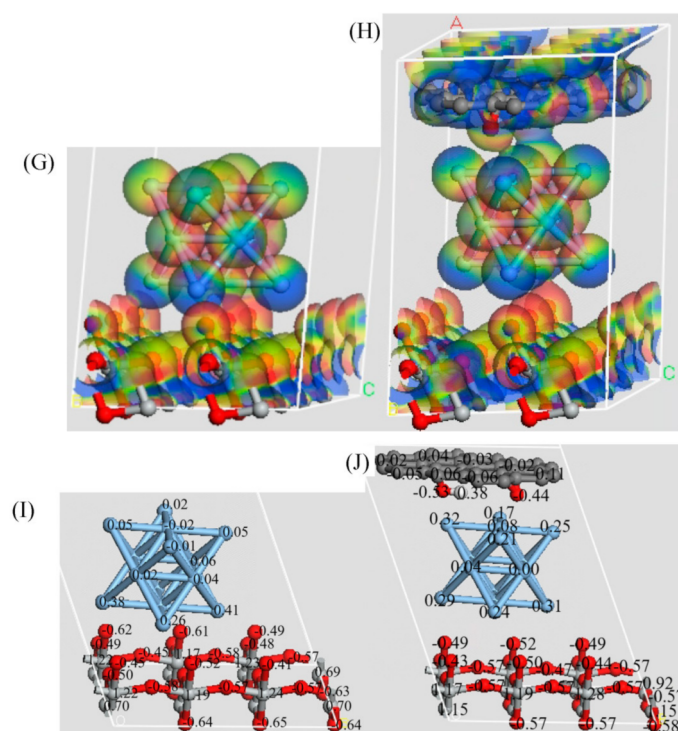


Figure 2. (A,B) Molecule structure models, (C,D) band structures, (E,F) total density of states, (G,H) charge density differences, and (I,J) Mulliken charge distributions of Ag/TiO₂ and GO/Ag/TiO₂ SERS substrates.

Figure 2C,D show band structures of the Ag/TiO₂ and GO/Ag/TiO₂ SERS substrates. Both band gaps of Ag/TiO₂ and GO/Ag/TiO₂ are close to zero, indicating highly electronic-conducting properties. This indicates that their band gaps are mostly dependent on the conducting Ag metal. Comparatively, GO/Ag/TiO₂ reveals more sufficient distribution levels of electron energy states above and below Fermi energy than does Ag/TiO₂, indicating more electron energy states within GO/Ag/TiO₂.

Figure 2E,F show total density of states (TDOS) of the Ag/TiO₂ and GO/Ag/TiO₂ SERS substrates. The TDOS curves of Ag/TiO₂ and GO/Ag/TiO₂ show that electron states cross from the valence band to the conducting band, indicating good electronic conductivity, which is consistent with the above result of band structures. Comparatively, GO/Ag/TiO₂ has a higher TDOS level at the Fermi energy of 0 eV in comparison with Ag/TiO₂, indicating more electron energy states for feasible electron transfer in GO/Ag/TiO₂.

Figure 2G,H show charge density differences of the Ag/TiO₂ and GO/Ag/TiO₂ SERS substrates. The polarization effect causes the partial potential distribution of atoms. Concerning the charge density difference of Ag/TiO₂, the oxygen atoms of TiO₂ present the negative charge and silver atoms present the positive charge at the interface between TiO₂ NTA and Ag nanoparticles, which leads to the electrostatic adsorption interaction of Ag/TiO₂. Concerning the charge density difference of GO/Ag/TiO₂, the oxygen atoms of GO present the negative charge and silver atoms present the positive charge at the interface between GO layers and Ag nanoparticles, which leads to additional electrostatic adsorption interaction of GO/Ag.

Figure 2I,J show the Mulliken charge distributions of the Ag/TiO₂ and GO/Ag/TiO₂ SERS substrates. Concerning the partial charge distribution of atoms in Ag/TiO₂, the negative charge of oxygen atoms in TiO₂ NTA ranges from -0.49 to -0.64 V. The positive charge of silver atoms in the Ag nanoparticles ranges from 0.04 to 0.41 V. Concerning the partial charge distribution of atoms in GO/Ag/TiO₂, the GO involves hydroxyl and epoxy groups, which keep a positive charge of $+0.38$ V for hydrogen and a negative charge from -0.44 to -0.53 V for oxygen. Additionally, GO also involves the positive charge of carbon

atoms, ranging from 0.04 to 0.11 V, and the negative charge of carbon atoms, ranging from -0.02 to -0.06 V. This Mulliken charge distribution result is consistent with the above charge–density difference, proving the formation of electrostatic interaction at the binary interfaces of GO/Ag/TiO₂.

Raman electromagnetic enhancement is mostly dependent on the microstructure of Ag nanoparticles in the GO/Ag/TiO₂ SERS substrate. In addition, Raman chemical enhancement is achieved by the charge transfer between the GO/Ag/TiO₂ NTA SERS substrate and the surface-adsorbed BPA molecule. Thus, the SERS sensor performance of GO/Ag/TiO₂ NTA is highly dependent on the surface adsorption and aggregation of organic molecules on its active SERS substrates. Figure 3 shows HOMO and LUMO frontier molecular orbital energy level diagrams of BPA/Ag on Ag/TiO₂ substrate and BPA/GO on GO/Ag/TiO₂ substrate. The BPA adsorption on the Ag/TiO₂ and GO/Ag/TiO₂ SERS substrates involves the interfacial interactions of BPA/Ag and BPA/GO. Concerning BPA/Ag, both the HOMO and LUMO frontier molecular orbital energy levels of BPA/Ag are located on Ag. The electron transfer between BPA and Ag is unlikely to occur in BPA/Ag, indicating the weak interfacial interaction of BPA adsorption on Ag/TiO₂. Comparatively, concerning BPA/GO, the HOMO molecular orbital energy level is located on GO and the LUMO molecular orbital energy level is located on BPA. The electron transfer between BPA and GO is likely to occur in BPA/GO, indicating the strong interfacial interaction of BPA adsorption on GO/Ag/TiO₂. In addition, the HOMO and LUMO energy levels of BPA/Ag are -0.1298 eV and -0.1159 eV, respectively. The corresponding HOMO–LUMO gap is 0.139 eV for BPA/Ag. Comparatively, the HOMO and LUMO energy levels of BPA/GO are -0.1624 eV and -0.1551 eV, respectively. The corresponding HOMO–LUMO gap is 0.073 eV for BPA/GO. This indicates the electron transfer is more feasible in BPA/GO than in BPA/Ag, which is highly ascribed to the strong interfacial adsorption between BPA and GO. It is believed that the promoted Raman chemical enhancement effect contributes to improving SERS sensing performance of the GO/Ag/TiO₂ NTA SERS substrate for the sensitive and accurate determination of BPA.

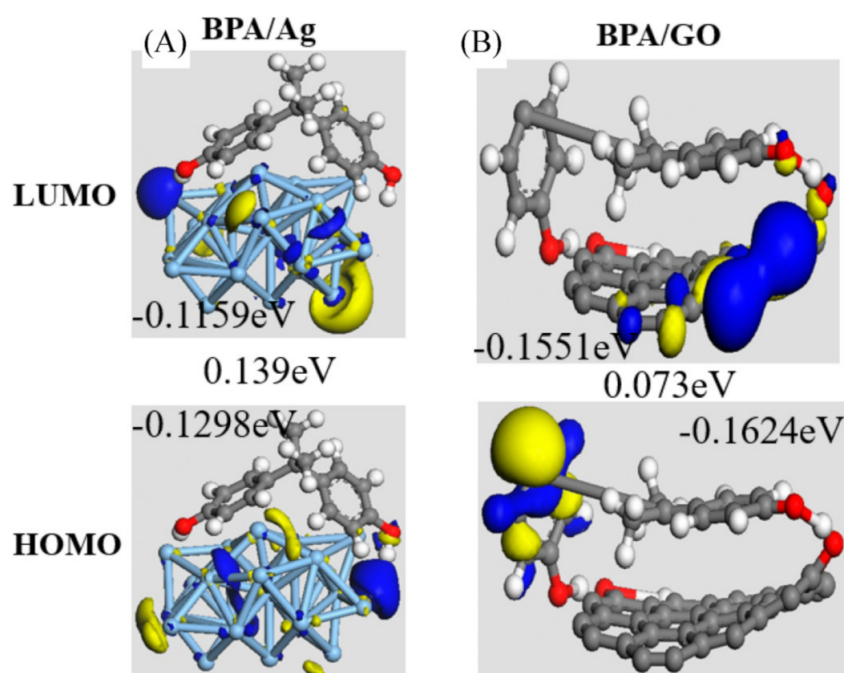


Figure 3. HOMO and LUMO frontier molecular orbital energy level diagrams of (A) BPA/Ag on Ag/TiO₂ substrate and (B) BPA/GO on GO/Ag/TiO₂ substrate.

The interfacial molecular interaction is regarded as a critical factor in influencing the molecule adsorption to the SERS substrates. The theoretical model calculation was carried

out to investigate the molecular interaction. Figure 4A,B shows the side view and top view of the optimized molecular structure model of BPA/GO. According to the DMol3 calculation result of geometry-structure optimization, two benzene rings of BPA keep a vertical arrangement, and the hexatomic carbon rings of GO keep a twisted arrangement. The H–O distance between the oxygen atom of the hydroxyl group in GO and the hydrogen atom of the hydroxyl group in BPA is 1.994 Å. Moreover, the H–O distance between the oxygen atom of the epoxy group in GO and the hydrogen atom of the hydroxyl group in BPA is 2.057 Å. Both H–O atomic distances fall into the hydrogen bonding range [12]. Therefore, the hydrogen-bonding interaction is well-established between BPA and GO in the BPA adsorption to the GO/Ag/TiO₂ NTA substrate. This result is consistent with the HOMO–LUMO band structure of BPA/GO.

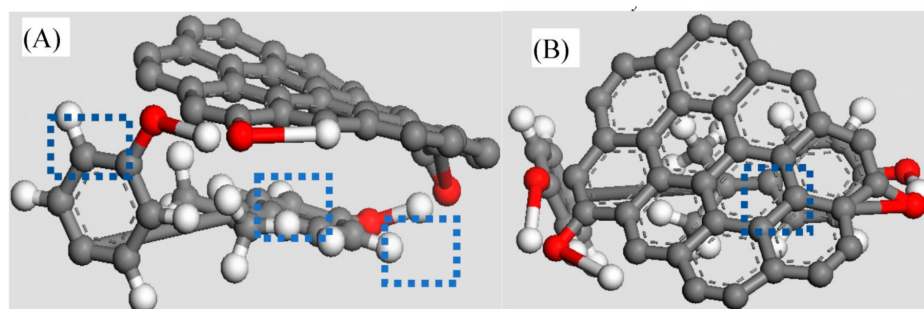


Figure 4. (A) Side view and (B) top view of the optimized molecular structure model of BPA/GO (● oxygen atom, ○ hydrogen atom, ● carbon atom).

The interfacial-bonding interaction of composite substrates is related to the SERS activity of the GO/Ag/TiO₂ NTA substrate, which can be used to evaluate the structural stability on the basis of the change of interfacial energy. According to the CASTEP calculation results, the surface energy of the individual components were determined to be −5880.65 eV for GO, −55,906.65 eV for Ag, and −29,595.59 eV for TiO₂. The final surface energies of multi-components were calculated to be −85,498.12 eV for Ag/TiO₂, −61,784.39 eV for GO/Ag, and −91,377.02 eV for GO/Ag/TiO₂. Thus, the declined surface energy was determined to be 4.12 eV for mono-interfaced Ag/TiO₂, 2.91 eV for mono-interfaced GO/Ag, and 5.87 eV for binary-interfaced GO/Ag/TiO₂. Ag/TiO₂, GO/Ag, and GO/Ag/TiO₂ all showed the lowered surface energy, which indicates the interfacial affinity of GO, Ag and TiO₂ to a certain degree. GO/Ag/TiO₂, with a much lower surface energy, presents a more stable structure and a higher affinity compared to Ag/TiO₂, which is highly ascribed to the intensified electrostatic interaction of binary interfaces on GO/Ag and Ag/TiO₂ in GO/Ag/TiO₂. This indicates that the binary interface of GO/Ag/TiO₂ involves more intensive bonding strength compared to the mono interface of Ag/TiO₂. Furthermore, concerning the interfacial adsorption between BPA molecules and SERS substrates, the declined surface adsorption energy of BPA was 4.32 eV for Ag/TiO₂ and 7.81 eV for GO/Ag/TiO₂. This indicates that the interfacial adsorption of BPA is much more feasible on the GO/Ag/TiO₂ substrate than on the Ag/TiO₂ substrate.

Figure 5A shows UV-vis spectra of 2.2×10^4 M BPA on the base of TiO₂, Ag/TiO₂ and GO/Ag/TiO₂ NTA SERS substrates. The characteristic UV absorption peaks of BPA are obviously declined due to the intensified adsorption of BPA on TiO₂, Ag/TiO₂, and GO/Ag/TiO₂ NTA substrates. Figure 5B shows the specific adsorption amounts of BPA on TiO₂, Ag/TiO₂, and GO/Ag/TiO₂ NTA SERS substrates. The specific adsorption amount of BPA was 3.3, 7.1, and 52.4 nmol cm^{−2} for TiO₂, Ag/TiO₂, and GO/Ag/TiO₂ NTA substrates, respectively. GO/Ag/TiO₂ NTA presents much higher adsorption capability than TiO₂ and Ag/TiO₂ NTA. This result is mostly ascribed to high interfacial affinity between GO and BPA, which has been proven by the theoretical calculation result of the more declined surface adsorption energy in GO/BPA. GO plays an important role on the interfacial adsorption of BPA. The π - π stacking interaction can be well-established between

benzene rings of the BPA molecule and hexatomic carbon rings of the GO molecule [32]. Furthermore, hydrogen bonds can be formed between the hydroxyl groups of GO and the hydroxyl groups of BPA [33]. Concerning strong surface adsorption and superior affinity between GO/Ag/TiO₂ NTA and BPA molecules, GO/Ag/TiO₂ NTA indeed exhibits a higher adsorption and aggregation capability of organic compound molecules, which, accordingly, contributes to higher SERS sensing activity.

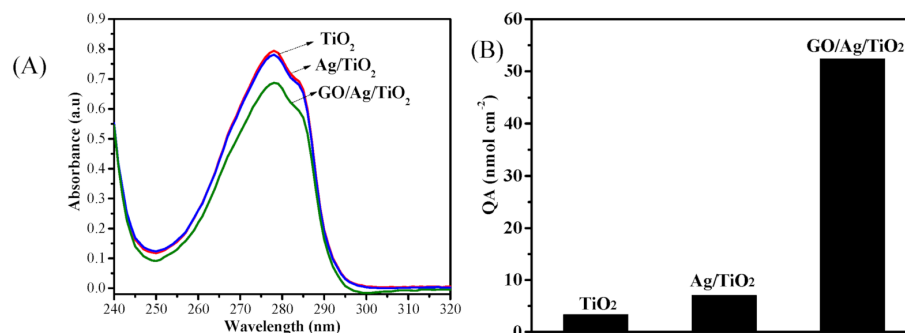


Figure 5. (A) UV-vis spectra of 2.2×10^{-4} M BPA on the base of TiO₂, Ag/TiO₂, and GO/Ag/TiO₂ NTA SERS substrates; (B) Specific adsorption amount on TiO₂, Ag/TiO₂, and GO/Ag/TiO₂ NTA SERS substrates.

GO/Ag/TiO₂ NTA was applied as a SERS sensor substrate for sensitive detection and determination of BPA. Figure 6A shows the Raman spectra of BPA with a concentration from 5×10^{-7} M to 5×10^{-4} M. The characteristic Raman peaks of BPA are observed, which are ascribed to phenyl ring vibration, C-C-C asymmetric stretching vibration, and =C-C bending vibration [34]. In addition, the characteristic Raman peaks of GO are also observed, which are ascribed to the D band and G band. The Raman-peak intensity of GO is unchanged. The characteristic Raman-peak intensity of BPA declines along with the decrease in BPA concentration, which is applied for SERS determination of BPA. Figure 6B shows characteristic Raman-peak intensity in terms of the BPA concentration curve of GO/Ag/TiO₂ SERS sensor for BPA determination. Such a SERS signal peak of BPA is still observed even at its low concentration of 5×10^{-7} M. This experimental result proves that the GO/Ag/TiO₂ NTA SERS substrate is suitable for determination of organic compound BPA.

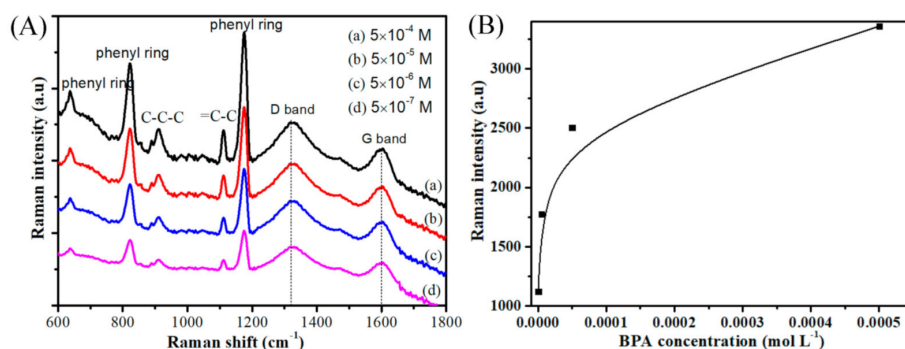


Figure 6. (A) Raman spectra and (B) characteristic Raman-peak intensity in terms of BPA concentration curve of GO/Ag/TiO₂ SERS sensor for BPA determination of (a) 5×10^{-4} M, (b) 5×10^{-5} M, (c) 5×10^{-6} M, and (d) 5×10^{-7} M.

4. Conclusions

GO/Ag/TiO₂ NTA was designed as an active SERS sensor substrate for sensitive determination of the organic compound bisphenol A. The experimental measurement and theoretical simulation calculation were adopted to investigate the sensing properties of the GO/Ag/TiO₂ NTA SERS substrate. The interfacial adsorption energy and interfacial

affinity energy were applied to investigate the interaction between the SERS substrate and organic molecule. The Raman spectrum response intensity and the electron transfer behavior were applied to investigate sensing activity of the GO/Ag/TiO₂ NTA SERS substrate. The specific adsorption amount of bisphenol A was 3.3, 7.1, and 52.4 nmol cm⁻² for TiO₂, Ag/TiO₂, and GO/Ag/TiO₂ NTA, respectively, presenting superior adsorption and aggregation capability of the bisphenol A molecule. The GO/Ag/TiO₂ NTA SERS sensor, accordingly, achieves the low detection limit of 5×10^{-7} M for bisphenol A. The density functional theory simulation calculation proves that GO/Ag/TiO₂ reveals a higher density of states, lower HOMO–LUMO gap, and stronger electrostatic interaction than does Ag/TiO₂, but exhibits similar electronic band gaps. Binary-interfaced GO/Ag/TiO₂ presents a more declined molecular structure surface energy of 5.87 eV, rather than 4.12 eV for mono-interfaced Ag/TiO₂. GO/Ag/TiO₂ also exhibits a more declined surface adsorption energy of 7.81 eV, rather than 4.32 eV for Ag/TiO₂, in the adsorption of bisphenol A. The simulation calculation verification results well confirm the superior performance of the GO/Ag/TiO₂ NTA SERS sensor for sensing detection and determination of organic compound bisphenol A. The superior SERS performance of the GO/Ag/TiO₂ NTA substrate is caused by the localized electromagnetic field enhancement of Ag nanoparticles, the charge-transfer chemical enhancement of GO, and the light-scattering enhancement of the highly aligned TiO₂ NTA microstructure.

Funding: This research received no external funding.

Institutional Review Board Statement: Not applicable.

Informed Consent Statement: Not applicable.

Data Availability Statement: Not applicable.

Acknowledgments: We thank the Big Data Computing Center of Southeast University for providing the facility support on the numerical calculations.

Conflicts of Interest: The author declares no conflict of interest.

References

1. Wang, J.; Anderson, W.; Li, J.; Lin, L.L.; Wang, Y.; Trau, M. A High-Resolution Study of in Situ Surface-Enhanced Raman Scattering Nanotag Behavior in Biological Systems. *J. Colloid Interface Sci.* **2019**, *537*, 536–546. [[CrossRef](#)] [[PubMed](#)]
2. Wang, Q.; Liu, L.; Wang, Y.; Liu, P.; Jiang, H.; Xu, Z.; Ma, Z.; Oren, S.; Chow, E.K.C.; Lu, M.; et al. Tunable Optical Nanoantennas Incorporating Bowtie Nanoantenna Arrays with Stimuli-Responsive Polymer. *Sci. Rep.* **2015**, *5*, 18567. [[CrossRef](#)] [[PubMed](#)]
3. Kozhina, E.P.; Bedin, S.A.; Nechaeva, N.L.; Podoynitsyn, S.N.; Tarakanov, V.P.; Andreev, S.N.; Grigoriev, Y.V.; Naumov, A.V. Ag-Nanowire Bundles with Gap Hot Spots Synthesized in Track-Etched Membranes as Effective Sers-Substrates. *Appl. Sci.* **2021**, *11*, 1375. [[CrossRef](#)]
4. Zhu, C.; Meng, G.; Zheng, P.; Huang, Q.; Li, Z.; Hu, X.; Wang, X.; Huang, Z.; Li, F.; Wu, N. A Hierarchically Ordered Array of Silver-Nanorod Bundles for Surface-Enhanced Raman Scattering Detection of Phenolic Pollutants. *Adv. Mater.* **2016**, *28*, 4871–4876. [[CrossRef](#)] [[PubMed](#)]
5. Tommasini, M.; Zanchi, C.; Lucotti, A.; Bombelli, A.; Villa, N.S.; Casazza, M.; Ciusani, E.; de Grazia, U.; Santoro, M.; Fazio, E.; et al. Laser-Synthesized Sers Substrates as Sensors toward Therapeutic Drug Monitoring. *Nanomaterials* **2019**, *9*, 677. [[CrossRef](#)] [[PubMed](#)]
6. Kozhina, E.P.; Andreev, S.N.; Tarakanov, V.P.; Bedin, S.A.; Doludenko, I.M.; Naumov, A.V. Study of Local Fields of Dendrite Nanostructures in Hot Spots Formed on Sers-Active Substrates Produced Via Template-Assisted Synthesis. *Bull. Russ. Acad. Sci. Phys.* **2020**, *84*, 1465–1468. [[CrossRef](#)]
7. Ding, S.-Y.; You, E.-M.; Tian, Z.-Q.; Moskovits, M. Electromagnetic Theories of Surface-Enhanced Raman Spectroscopy. *Chem. Soc. Rev.* **2017**, *46*, 4042–4076. [[CrossRef](#)] [[PubMed](#)]
8. McNeely, J.; Ingraham, H.M.; Premasiri, W.R.; Ziegler, L.D. Chemical Enhancement Effects on Protoporphyrin IX Surface-Enhanced Raman Spectra: Metal Substrate Dependence and a Vibronic Theory Analysis. *J. Raman Spectrosc.* **2021**, *52*, 323–338. [[CrossRef](#)]
9. Xie, Y. Electrochemical Properties of Sodium Manganese Oxide/Nickel Foam Supercapacitor Electrode Material. *Inorg. Nano-Met. Chem.* **2022**, *52*, 548–555. [[CrossRef](#)]
10. Harris, R.A.; Prakash, J. Surface Enhanced Raman Scattering with Methyl-Orange on Ag-TiO₂ Nanocomposites: A Computational Investigation. *J. Mol. Graph. Modell.* **2019**, *87*, 220–226. [[CrossRef](#)]

11. Xie, Y. Enhancement Effect of Silver Nanoparticles Decorated Titania Nanotube Array Acting as Active Sers Substrate. *Inorg. Nano-Met. Chem.* **2021**, *Published Online*. [[CrossRef](#)]
12. Xie, Y. Electrochemical Performance of Polyaniline Support on Electrochemical Activated Carbon Fiber. *J. Mater. Eng. Perform.* **2022**, *31*, 1949–1955. [[CrossRef](#)]
13. Xie, Y. Electrochemical and Hydrothermal Activation of Carbon Fiber Supercapacitor Electrode. *Fibers Polym.* **2022**, *23*, 10–17. [[CrossRef](#)]
14. Lin, L.-K.; Stanciu, L.A. Bisphenol a Detection Using Gold Nanostars in a Sers Improved Lateral Flow Immunochromatographic Assay. *Sens. Actuators B Chem.* **2018**, *276*, 222–229. [[CrossRef](#)]
15. Wang, Y.; Xie, Y. Sandwich-Structured Polypyrrole Layer/Kcl-Polyacrylamide-Gelatin Hydrogel/Polypyrrole Layer as All-in-One Polymer Self-Healing Supercapacitor. *Electrochim. Acta* **2022**, *435*, 141371. [[CrossRef](#)]
16. Wang, H.; Xie, Y. Hydrogen Bond Enforced Polyaniline Grown on Activated Carbon Fibers Substrate for Wearable Bracelet Supercapacitor. *J. Energy Storage* **2022**, *52*, 105042. [[CrossRef](#)]
17. Xie, Y. Electrochemical Investigation of Free-Standing Reduced Graphene Oxide Hydrogel. *Fuller. Nanotub. Carbon Nanostructures* **2022**, *30*, 619–625. [[CrossRef](#)]
18. Yan, H.; Wu, H.; Li, K.; Wang, Y.W.; Tao, X.; Yang, H.; Li, A.M.; Cheng, R.S. Influence of the Surface Structure of Graphene Oxide on the Adsorption of Aromatic Organic Compounds from Water. *ACS Appl. Mater. Interfaces* **2015**, *7*, 6690–6697. [[CrossRef](#)]
19. Almohammed, S.; Zhang, F.; Rodriguez, B.J.; Rice, J.H. Electric Field-Induced Chemical Surface-Enhanced Raman Spectroscopy Enhancement from Aligned Peptide Nanotube-Graphene Oxide Templates for Universal Trace Detection of Biomolecules. *J. Phys. Chem. Lett.* **2019**, *10*, 1878–1887. [[CrossRef](#)]
20. Kostadinova, T.; Politakos, N.; Trajcheva, A.; Blazevska-Gilev, J.; Tomovska, R. Effect of Graphene Characteristics on Morphology and Performance of Composite Noble Metal-Reduced Graphene Oxide Sers Substrate. *Molecules* **2021**, *26*, 4775. [[CrossRef](#)]
21. Fang, H.; Zhang, C.X.; Liu, L.; Zhao, Y.M.; Xu, H.J. Recyclable Three-Dimensional Ag Nanoparticle-Decorated TiO₂ Nanorod Arrays for Surface-Enhanced Raman Scattering. *Biosens. Bioelectron.* **2015**, *64*, 434–441. [[CrossRef](#)] [[PubMed](#)]
22. Samodelova, M.V.; Kapitanova, O.O.; Evdokimov, P.V.; Eremina, O.E.; Goodilin, E.A.; Veselova, I.A. Plasmonic Features of Free-Standing Chitosan Nanocomposite Film with Silver and Graphene Oxide for Sers Applications. *Nanotechnology* **2022**, *33*, 335501. [[CrossRef](#)] [[PubMed](#)]
23. Xie, Y.; Meng, Y. Sers Performance of Graphene Oxide Decorated Silver Nanoparticle/Titania Nanotube Array. *RSC Adv.* **2014**, *4*, 41734–41743. [[CrossRef](#)]
24. Wang, Z.; Li, S.; Wang, J.; Shao, Y.; Mei, L. A Recyclable Graphene/Ag/TiO₂ Sers Substrate with High Stability and Reproducibility for Detection of Dye Molecules. *New J. Chem.* **2022**, *46*, 18787–18795. [[CrossRef](#)]
25. Doan, M.Q.; Anh, N.H.; Van Tuan, H.; Tu, N.C.; Lam, N.H.; Khi, N.T.; Phan, V.N.; Thang, P.D.; Le, A.-T. Improving Sers Sensing Efficiency and Catalytic Reduction Activity in Multifunctional Ternary Ag-TiO₂-Go Nanostructures: Roles of Electron Transfer Process on Performance Enhancement. *Adsorpt. Sci. Technol.* **2021**, *2021*, 1169599. [[CrossRef](#)]
26. Deriu, C.; Morozov, A.N.; Mebel, A.M. Direct and Water-Mediated Adsorption of Stabilizers on Sers-Active Colloidal Bimetallic Plasmonic Nanomaterials: Insight into Citrate-Auag Interactions from Dft Calculations. *J. Phys. Chem. A* **2022**, *126*, 5236–5251. [[CrossRef](#)]
27. Muniz-Miranda, F.; Pedone, A.; Menziani, M.C.; Muniz-Miranda, M. Dft and Td-Dft Study of the Chemical Effect in the Sers Spectra of Piperidine Adsorbed on Silver Colloidal Nanoparticles. *Nanomaterials* **2022**, *12*, 2907. [[CrossRef](#)]
28. Premkumar, R.; Hussain, S.; Jayram, N.D.; Koyambo-Konzapa, S.-J.; Revathy, M.S.; Mathavan, T.; Benial, A.M.F. Adsorption and Orientation Characteristics of 1-Methylpyrrole-2-Carbonyl Chloride Using Sers and Dft Investigations. *J. Mol. Struct.* **2022**, *1253*, 132201. [[CrossRef](#)]
29. Wu, X.; Vega Canamares, M.; Kakoulli, I.; Sanchez-Cortes, S. Chemical Characterization and Molecular Dynamics Simulations of Bufotenine by Surface-Enhanced Raman Scattering (Sers) and Density Functional Theory (Dft). *J. Phys. Chem. Lett.* **2022**, *13*, 5831–5837. [[CrossRef](#)]
30. Ricci, M.; Becucci, M.; Castellucci, E.M. Chemical Enhancement in the Sers Spectra of Indigo: Dft Calculation of the Raman Spectra of Indigo-Ag₁₄ Complexes. *Vib. Spectrosc.* **2019**, *100*, 159–166. [[CrossRef](#)]
31. Chen, J.; Huang, X.; Ye, R.; Huang, D.; Wang, Y.; Chen, S. Fabrication of a Novel Electrochemical Sensor Using Conductive Mof Cu-Cat Anchored on Reduced Graphene Oxide for Bpa Detection. *J. Appl. Electrochem.* **2022**, *52*, 1617–1628. [[CrossRef](#)]
32. Zhang, J.; Lu, X.; Shi, C.; Yan, B.; Gong, L.; Chen, J.; Xiang, L.; Xu, H.; Liu, Q.; Zeng, H. Unraveling the Molecular Interaction Mechanism between Graphene Oxide and Aromatic Organic Compounds with Implications on Wastewater Treatment. *Chem. Eng. J.* **2019**, *358*, 842–849. [[CrossRef](#)]
33. Xu, J.; Wang, L.; Zhu, Y.F. Decontamination of Bisphenol a from Aqueous Solution by Graphene Adsorption. *Langmuir* **2012**, *28*, 8418–8425. [[CrossRef](#)] [[PubMed](#)]
34. Liu, S.; Cui, R.; Ma, Y.; Yu, Q.; Kannegulla, A.; Wu, B.; Fan, H.; Wang, A.X.; Kong, X. Plasmonic Cellulose Textile Fiber from Waste Paper for Bpa Sensing by Sers. *Spectrochim. Acta Part A* **2020**, *227*, 117664. [[CrossRef](#)]